Research article

Identification and confirmation of 14-3-3 ζ as a novel target of ginsenosides in brain tissues

Feiyan Chen [a, b, 1], Lin Chen [d, 1], Weifeng Liang [b], Zhengguang Zhang [b], Jiao Li [b], Wan Zheng [b], Zhu Zhu [e], Jiapeng Zhu [b, *], Yunan Zhao [c, **]

[a] Research and Innovation Center, College of Traditional Chinese Medicine Integrated Chinese and Western Medicine College, Nanjing University of Chinese Medicine, Nanjing, China
[b] Department of Cell Biology and Medical Genetics, School of Medicine & Holistic Integrative Medicine, Nanjing University of Chinese Medicine, Nanjing, China
[c] Department of Pathology and Pathophysiology, School of Medicine & Holistic Integrative Medicine, Nanjing University of Chinese Medicine, Nanjing, China
[d] Department of Physiology, School of Medicine & Holistic Integrative Medicine, Nanjing University of Chinese Medicine, Nanjing, China
[e] Department of Pharmacology, School of Medicine & Holistic Integrative Medicine, Nanjing University of Chinese Medicine, Nanjing, China

ARTICLE INFO

ABSTRACT

Background: Ginseng can help regulate brain excitability, promote learning and memory, and resist cerebral ischemia in the central nervous system. Ginsenosides are the major effective compounds of Ginseng, but their protein targets in the brain have not been determined.

Methods: We screened proteins that interact with the main components of ginseng (ginsenosides) by affinity chromatography and identified the 14-3-3 ζ protein as a potential target of ginsenosides in brain tissues.

Results: Biolayer interferometry (BLI) analysis showed that 20(S)-protopanaxadiol (PPD), a ginseng saponin metabolite, exhibited the highest direct interaction to the 14-3-3 ζ protein. Subsequently, BLI kinetics analysis and isothermal titration calorimetry (ITC) assay showed that PPD specifically bound to the 14-3-3 ζ protein. The cocrystal structure of the 14-3-3 ζ protein-PPD complex showed that the main interactions occurred between the residues R56, R127, and Y128 of the 14-3-3 ζ protein and a portion of PPD. Moreover, mutating any of the above residues resulted in a significant decrease of affinity between PPD and the 14-3-3 ζ protein.

Conclusion: Our results indicate the 14-3-3 ζ protein is the target of PPD, a ginsenoside metabolite. Crystallographic and mutagenesis studies suggest a direct interaction between PPD and the 14-3-3 ζ protein. This finding can help in the development of small-molecular compounds that bind to the 14-3-3 ζ protein on the basis of the structure of dammarane-type triterpenoid.

1. Introduction

Ginseng is one of the most widely consumed herbal nutritional products in the world [1]. Pharmacological studies showed that ginseng contains various chemical components, including ginsenosides, ginseng polysaccharides, peptides, fatty acids, and amino acids [2]. Ginsenosides are the primary active components of ginseng and various ginsenosides have been identified and isolated. According to the chemical structure of their aglycones, ginsenosides can be mainly divided into two categories, namely, the protopanaxadiol (e.g., Rb2, Rb1, Rd, Rc, Rh2, and Rg3) and protopanaxatriol groups (e.g., Re, Rg1, Rf, and Rh1) [3]. The original form of ginsenosides can be metabolized by intestinal bacteria and liver metabolism, mainly into deglucose-based sub-saponins or aglycones [4,5]. In the protopanaxatriol group, Re and Rg1 are biotransformed into 20(S)-protopanaxatriol (PPT) via F1 and Rh1. In the protopanaxadiol group, Rd and Rb1 are converted into 20(S)-protopanaxadiol (PPD) by ginsenoside compound K (CK) and Rh2 [6,7]. After oral administration, ginsenosides and their metabolites are absorbed through the intestinal tract into the systemic circulation. Previous studies have shown that ginsenosides could

* Corresponding author. Department of Cell Biology and Medical Genetics, School of Medicine & Holistic Integrative Medicine, Nanjing University of Chinese Medicine, Nanjing, 210046, China.
** Corresponding author. Department of Pathology and Pathophysiology, School of Medicine & Holistic Integrative Medicine, Nanjing University of Chinese Medicine, Nanjing, 210046, China
E-mail addresses: zhujiapeng@hotmail.com (J. Zhu), zhaoyunan-js@163.com (Y. Zhao).
[1] These authors contributed equally to this work.

penetrate the blood−brain barrier (BBB), directly target the neurons, and may cause pharmacological effects in the central nervous system (CNS). For instance, through rapid HPLC-MS/MS analysis, Liu et al [8] found the distribution of ginsenosides Rg1, Re, Rb1, Rc, and Rd in brain tissues after intravenous injection of ginseng extracts. As for the aglycones of ginsenosides, the low water solubility of PPD resulted in poor oral bioavailability and limited its effective delivery to the brain. However, compared with unformulated PPD, the prepared nanocrystals can significantly improve PPD's oral bioavailability and drug concentration in the brain after oral administration in rats [9,10].

Ginseng affects the nervous system, and ginsenosides have a neuroprotective effect and enhance cognitive performance and memory [11]. Nowadays, ginsenosides have become a research hotspot in the treatment of nervous system diseases because of their effectiveness, low toxicity and minor side effects. For example, ginsenoside Rg1 has good antiaging effects [12]. Ginsenosides Rh2 and Rg3 are promising low-toxic candidates for cancer prevention and treatment [13]. Ginsenoside Ro considerably suppresses tumor growth with out significant side effects on immune organs and body weight [14]. At present, a large number of studies have proved that ginsenosides have positive pharmacological effects on the CNS. Zhang et al [15] reported that ginsenoside Rb3 and its four deglycosylated derivatives- Rg3, Rh2, CK, and PPD - have antidepressant activities in mice models. Chen et al [16] showed that ginsenoside Rb1 vigorously prevents loss in the integrity of BBB after cerebral ischemia by negatively regulating NOX4-derived reactive oxygen species (ROS) production and local inflammation. Zhu et al [17] proved that Rg1 may be a useful compound to prevent age-related impairment related to learning and memory. Hou et al [18] demonstrated that long-term Rh2 administration might contribute to spatial learning by enhancing the role of newly generated hippocampal cells in the dentate gyrus (DG) of mice or a parallel mechanism of the enriched environment. However, the immediate protein target of ginsenosides in the brain remains unknown.

To identify the protein targets for ginsenosides in brain tissues, we fixed ginsenosides to 4% cross-linked agarose beads with covalent-linked diamino dipropylamine, and used affinity chromatography which is a classic target recognition method [19]. From the initial screening, we identified five proteins as potential targets for ginsenosides in brain tissues, including the 14-3-3 ζ protein, the 14-3-3 ε protein, actin, creatine kinase B-type, and ATP synthase subunit beta, among which the 14-3-3 ζ protein was further studied. We applied BLI to detect the direct interaction of ginsenosides and the 14-3-3 ζ protein and found that their metabolite PPD displayed the strongest direct interaction with 14-3-3 ζ protein. The interaction of PPD with 14-3-3 ζ protein was proved through BLI and ITC assay. X-ray crystallography and site-directed mutagenesis analysis identified the binding sites between PPD and the 14-3-3 ζ protein.

2. Methods

2.1. Extraction of high-purity ginseng total saponins

High-purity ginseng total saponins were extracted as previously described [3,20]. In brief, the ginsenosides Re, Rh1, Rg2, Rg1, Rb2, Rc, Rg3, F1, Rd, and Rb3 were measured in high-purity ginseng total saponins (Supplementary Figure 1). According to the colorimetric method and the charged electrosol detection response, the estimated total saponin contents were approximately 107% and 90%, respectively [21]. Re, Rg1, Rb1, F1, Rh1, Rh2, CK, PPD , Rd, and PPT standards (purity ≥98%) were obtained from the National Institute of Food and Drug Control (Beijing, China).

2.2. Experimental animals

The mice needed for brain tissue were obtained from SLAC Laboratory Animal Co., Ltd. (Shanghai, China). All animal procedures were approved by the Institutional Animal Care and Use Committee of Nanjing University of Chinese Medicine and carried out in accordance with the Guidelines of Accommodation and Care for Animals formulated by the Chinese Convention for the Protection of Vertebrate Animals Used for Experimental and Other Scientific Purposes. The minimum number of animals required to obtain consistent data were used.

2.3. Affinity chromatography

The ginsenoside-bead conjugate was synthesized as described previously [22], with minor modifications. The detailed steps are described in the Supplementary Methods.

2.4. Cloning and protein expression

The construct containing the 14-3-3ζ gene was generated by PCR from the human genome, and a hexahistidine tag was added to the N-terminus of the gene, followed by a TEV cleavage site. The gene was subcloned into the pET28a vector and transformed into *Escherichia coli* BL21(DE3). The transformed BL21(DE3) cells were grown in Luria-Bertani medium containing 50 μg/ml Kanamycin at 37 °C until the OD600 reached approximately 0.6. Then, the temperature was changed to 25 °C and *E.coli* cells were induced with isopropyl-d-1-thiogalactopyranoside (IPTG) to a final concentration of 0.5 mM for 18 h [23].

2.5. Protein purification

The detailed procedures of protein purification are described in the Supplementary Methods. After purification of nickel column, the 14-3-3 ζ protein was digested overnight at 4 °C with TEV protease at a ratio of 1:30 (protease : protein) [24] to remove the label. Under denaturing conditions, the molecular weight was estimated using a protein marker (Bio-Rad, California, USA) as a reference protein, and protein purity was evaluated by sodium lauryl sulfate-polyacrylamide gel electrophoresis (SDS-PAGE) on a 15% polyacrylamide gel (Supplementary Figure 2). The concentration of 14-3-3 ζ protein was then detected at the absorbance of 280 nm by using a molar absorptivity constant calculated using the ExPASy/ProtParam tool (https://web.expasy.org/protparam/) [25].

2.6. Site-directed mutagenesis

The open reading frame (ORF) of 14-3-3 ζ was amplified using the cDNA of HCM cells (BeNa Culture Collection, Beijing, China) as a template and the primers (Supplementary Table1). The amplicon of 14-3-3 ζ was digested with BamHII and SalI, and then cloned into SalI /BamHI -digested expression vector *pET28a* to generate pET-14-3-3 ζ. Using site-directed mutagenesis with pET-14-3-3 ζ as template, we constructed pET56, pET127 and pET128, which have mutations of arginine at position 56 to alanine (14-3-3 ζ R56A, Mutant 1, Supplementary Figure 3), arginine at position 127 to alanine (14-3-3 ζ R127A, Mutant 2, Supplementary Figure 4) and tyrosine at position 128 to alanine (14-3-3 ζ Y128A, Mutant 3, Supplementary Figure 5) , respectively [3]. The detailed steps are described in the Supplementary Methods.

2.7. Biolayer interferometry

The binding affinities between PPD and WT or the mutants of human 14-3-3 ζ protein were measured using the BLI technique for testing. Measurements were carried out at 30 °C as previously described [26]. The detailed process is described in the Supplementary Methods. The final K_{on} and K_{off} rate constants were used to calculate the affinity of protein and small molecule ($K_D = K_{off}/K_{on}$). All experiments were repeated in thrice.

2.8. Isothermal Titration Calorimetry

ITC experiments were executed using a VP-ITC instrument (MicroCal, Northampton, MA) [27]. The detailed process is described in the Supplementary Methods. The K_D values listed represent the average of at least three independent measurements.

2.9. Protein crystallization and structural elucidation

Crystallization was performed using the sitting drop vapor diffusion method. Exactly 10 mg/ml 14-3-3 ζ was incubated with PPD in a molar ratio of 1:10 at room temperature for 1 h. Moreover, 0.3 μL of proteisolution containing 10 mg/ml 14-3-3 ζ and 5 mg/ml PPD in 50 mM NaCl , and 20 mM Tris at pH 8.0 was mixed with 0.3 μL of well solution containing 0.1 M sodium citrate tribasic dehydrate at pH 5.6, 0.2 M ammonium acetate, and 30% w/v PEG 4000. The crystallization drop was incubated at 290 K against 40 μL of well solution. The crystals of 14-3-3 ζ-PPD complex appeared in one day and reached the maximum size of 150 μm × 100 μm × 80 μm after seven days. The cyrstals were directly flash-frozen in liquid nitrogen. Diffraction data were collected from the beamline BL17U1 of the Shanghai Synchrotron Radiation Facility (SSRF) at 100 K [28]. Images were processed with imosflm [29]. The structure of the 14-3-3ζ-PPD complex was resolved through molecular replacement implemented in Phaser [30]. The coordinates of the structure (PDB code: 6ejl) were used as a search model. Then, the model was briefly refined using Phenix [31] and then manually adjusted using Coot [32]. The final model was refined to R_{free}=0.2772. All crystallographic figures were created using PYMOL (http:// www.pymol.org/) [25].

2.10. Statistical analysis

The data in this study were expressed as the mean of the number of experiments shown ± the standard error of the mean (S.E.M.) and analyzed using the statistical software package of Social Science Statistics Software Package version 10.1.

3. Results

3.1. Primary screening for the protein targets of ginsenosides in brain tissues by affinity chromatography

High-purity ginseng total saponins were used as ligands, and their glycosyl group was used to attach to the resin by oxidation with sodium periodate (Fig. 1A). The beads attached to the saponins were then incubated with the brain tissue extracts and washed extensively to remove non-specifically bound proteins. Tightly bound proteins were eluted under high denaturing conditions and analyzed by SDS-PAGE (Fig. 1B). The results showed that two protein strips (Bands 1 and 3) in the brain tissues had a certain affinity with the control resin, and 10 protein strips (Bands 1 ~ 10) had a certain affinity with the attached resin in the ginseng total saponin (Fig. 2A). Bands 2 and 4 ~ 10 were analyzed by mass spectrometry. Bands 4 ~ 8 were successfully identified using the Mascot search engine, and the results are shown in Supplementary Figures 6-10. The potential target proteins of the top Mascot score for each band were 14-3-3 protein zeta (Supplementary Figure 11), 14-3-3 protein epsilon (Supplementary Figure 12), actin (Supplementary Figure 13), creatine kinase B-type (Supplementary Figure 14), and ATP synthase subunit beta (Supplementary Figure 15) (Fig. 2B). The direct interaction between ginsenosides and 14-3-3 ζ was considered as a priority in subsequent research.
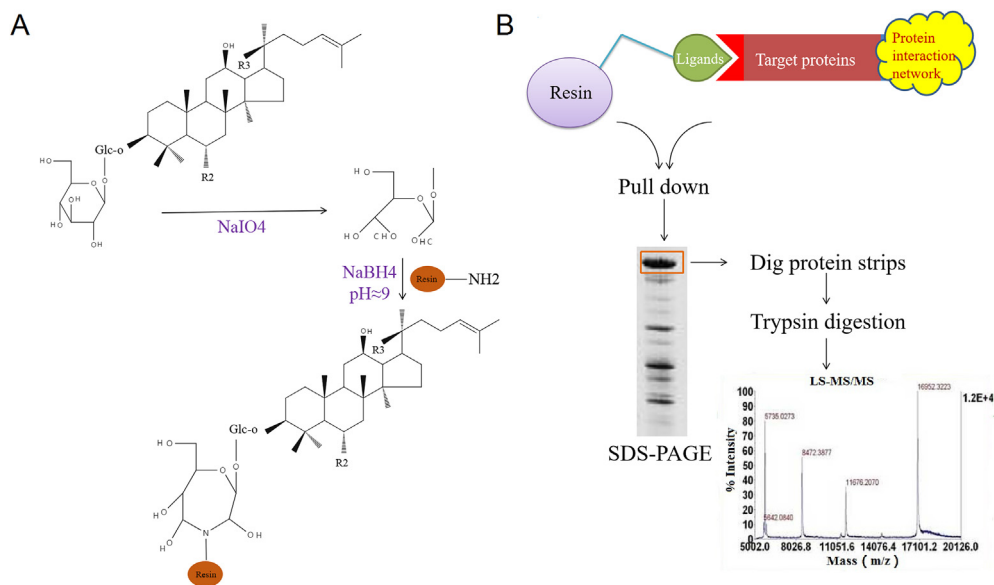

Fig. 1. General experimental procedure for affinity chromatography of small molecule. **(A)** Sodium periodate oxidation method is used to immobilize ginsenosides on the resin. **(B)** To enrich target proteins, we incubated protein lysates with the matrix-ligand chemical complex. Sodium dodecyl sulfate polyacrylamide gel electrophoresis (SDS-PAGE) and liquid chromatography coupled with tandem mass spectrometry (LC-MS/MS) analysis were used to detect the target proteins in the elution mixture.
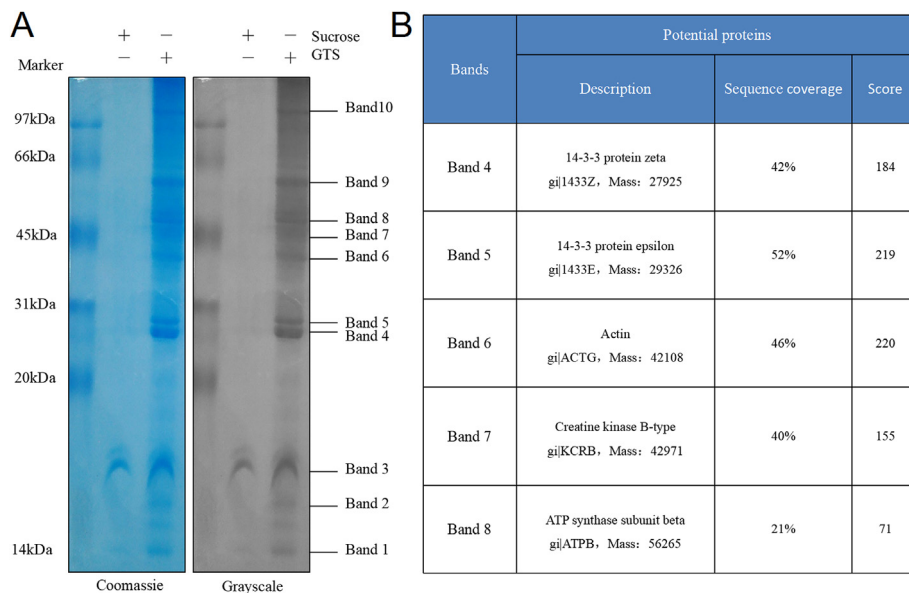
Fig. 2. Affinity chromatography was used to identify the protein target of ginsenosides in brain tissues. (**A**) Ginseng total saponins (GTS) were used as the ligand, while the negative control pull-down adopted sucrose was used as the ligand. SDS-PAGE coupled with Coomassie blue staining was used to visualize the eluted mixtures. Bands of varying abundance between GTS and control samples were excised and then identified by LC-MS/MS. (**B**) Mass spectrometry data were converted into a format of Mascot universal and then resolved via the Mascot search engine to recognize proteins from the database of peptide sequence. Based on the sequence coverage and Mascot score, the most potential proteins for each band were listed.
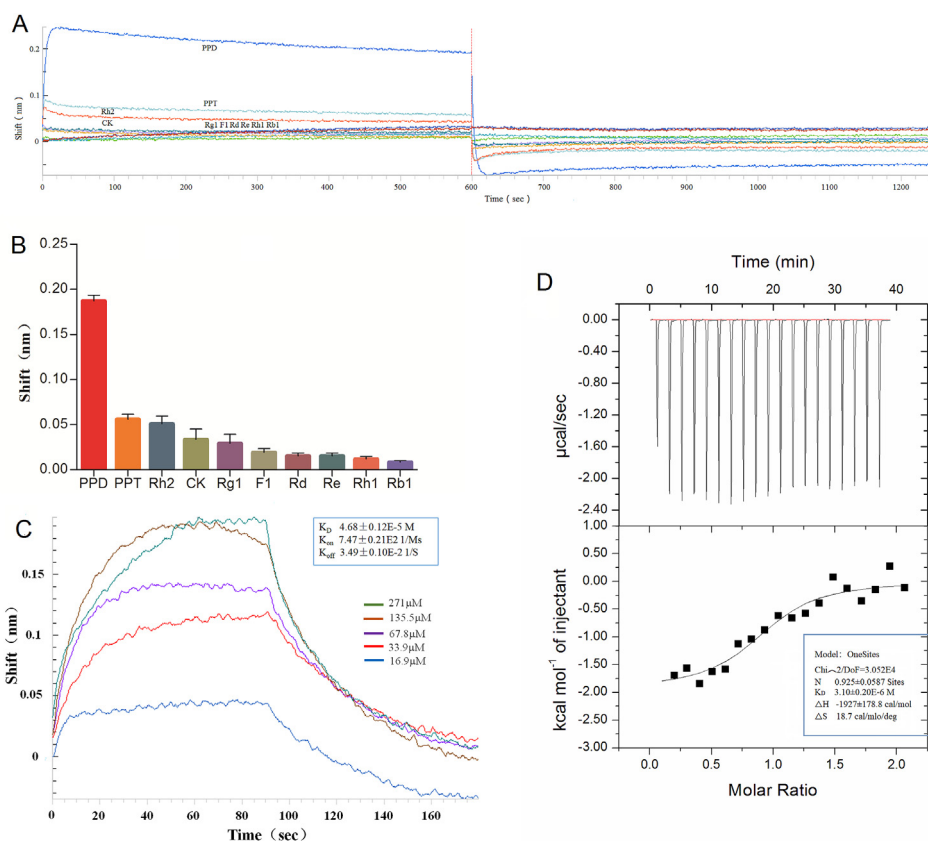

Fig. 3. Interaction of 14-3-3 ζ protein with ginsenosides. (**A**) The representative association and dissociation curves of the 14-3-3 ζ protein to ginsenosides and aglycones (PPD and PPT) were obtained by BLI analysis. (**B**) The direct binding reaction of the 14-3-3 ζ protein with ginsenosides and aglycones (PPD and PPT) were measured using the BLI technology (mean ± SEM, $n = 3$). (**C**) PPD binding to human 14-3-3 ζ protein was observed by BLI kinetic analysis. The PPD concentrations were set to 16.9, 33.9, 67.8, 135.5 and 271 μM. The results were obtained from at least three experiments. (**D**) ITC analysis for the 14-3-3 ζ protein binding to PPD. The ITC data displayed represents three replicates, and fitting errors are reported. PPD, 20(S)-protopanaxadiol; PPT, protopanaxatriol; SEM, standard error of mean.
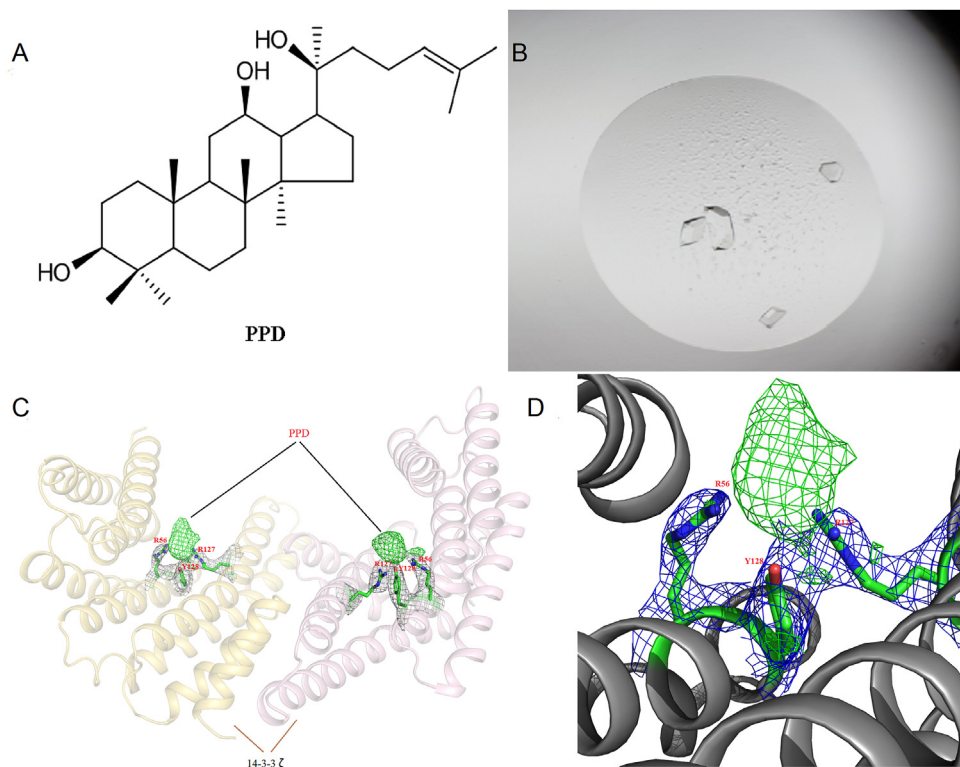
Fig. 4. Co-crystal structure of PPD and 14-3-3 ζ protein. (**A**) The chemical structure for PPD shows a co-crystal with the 14-3-3 ζ protein. (**B**) Crystals of the PPD-14-3-3 ζ complex. (**C**) Electron density (2Fo-Fc green mesh) of small molecule PPD bound to 14-3-3 ζ protein (yellow and pink cartoon). Residues of 14-3-3 ζ protein that are important for direct contacts with the PPD are shown as sticks. (**D**) Final 2Fo-Fc electron density map of PPD (green mesh; contoured at 1σ).

3.2. PPD bound directly to the 14-3-3 ζ protein

First, direct binding was measured by BLI, where human 14-3-3 ζ was fixed on a biosensor, and the wavelength shift was detected in real time after adding or diluting small molecules. At a concentration of 271μM, the direct binding response of 14-3-3 ζ to Re, Rg1, Rb1, Rh1, Rd,F1, GK, Rh2, PPD , and PPT is shown in Fig. 3A and B. Ginsenosides including Rb1, Rh1, Rd, Re, and F1 barely interacted with the 14-3-3 ζ protein. Rg1, CK, Rh2, and the aglycones (PPD and PPT) exhibited significant affinity to the 14-3-3 ζ protein. Among these compounds, PPD had the strongest binding activity to the 14-3-3 ζ protein and was used for subsequent affinity and binding conformational analysis.

The ratios of intermolecular K_{on}, K_{off}, and binding constants ($K_D = K_{off}/K_{on}$) were determined using BLI technique [33]. The BLI kinetics analysis suggested that the affinity (K_D) of PPD for 14-3-3ζ protein was 4.68 ± 0.12E-5 M. The K_{on} and K_{off} ratios of the 14-3-3ζ protein to PPD were 7.47 ± 0.21E2 1/Ms and 3.49 ± 0.10E-2 1/s, respectively (Fig. 3C). To further verify the direct interaction of 14-3-3 ζ to PPD and assess the physicochemical parameters of this interaction, we performed ITC analysis to detect the affinity of the binding partners in their natural states [34]. Exactly 271μM of PPD was titrated into 50μM of 14-3-3 ζ protein. The affinity K_D of the PPD to 14-3-3 ζ was 3.10 ± 0.20E-6 M, as measured by three independent experiments and calculated with a very suitable 1:1 binding model. The thermodynamic parameters for the interaction suggest that it is driven by helium and has a low entropy component ($\Delta H = -1927 \pm 178.8$ cal/mol , $\Delta S = 18.7$cal/mol/deg) (Fig. 3D).

3.3. Crystallographic study of the PPD−14-3-3 ζ complex

Co-crystallization of the 14-3-3 ζ protein with PPD (Fig. 4A) yielded the best crystal that diffracted to a resolution of 2.6 Å (Fig. 4B) and belonged to the space group P212121, with unit-cell parameters of $a = 70.045$, $b = 72.259$, and $c = 129.312$ (Table 1).

Table 1
Data Collection and refinement statistics for the 14-3-3 ζ and PPD complex. Statistics for the highest-resolution shell are shown in parentheses

Data collection	
Wavelength (Å)	0.9793
Space group	P 21 21 21
Unit cell	a=70.045, b= 72.259, c= 129.312
Resolution range	27.19-2.6 (2.693-2.6)
Total reflections	132049 (13171)
Unique reflections	20767 (2034)
R-merge	0.07037 (1.112)
Mean I/sigma(I)	11.96 (1.18)
Multiplicity	6.4 (6.5)
Completeness (%)	98.82 (99.71)
CC1/2	0.998 (0.804)
Refinement	
R-work	0.2364 (0.5052)
R-free	0.2772 (0.4969)
Number of non-hydrogen atoms	3646
macromolecules	3646
Protein residues	460
R.m.s.d	
Bond lengths (Å)	0.004
Bond angles	0.86
Ramachandran plot	
Favored (%)	97.15
Allowed (%)	2.63
Outliers (%)	0.22
Average B-factor	125.54

By using the previously reported structure of the 14-3-3-ASK1 fusion protein (PDB entry 6ejl) as a search model, the structure was determined by molecular replacement. A final R_{work} of 0.2364 and R_{free} of 0.2772 were refined to the model. Table 1 summarizes the details of data collection and optimization statistics.

3.4. Crystal structure of the PPD−14-3-3 ζ complex

The crystal structure suggests the 14-3-3 ζ protein formed a homodimer(Fig. 4C). The initial Fo-Fc map shows extra density near the residues Arg56, Arg127 and Tyr128, suggesting the position of the bound PPD. However, considering the relatively weak interaction, the electron density was not clear enough to locate the exact position of the individual atoms of the PPD molecule (Fig. 4D).

3.5. R56, R127, and Y128 residues were critical sites for the interaction of 14-3-3 ζ protein with PPD

According to the crystal structure of 14-3-3 ζ protein with PPD, we generated a series of mutants of the 14-3-3 ζ proteins R56A, R127A, and Y128A (Fig. 5A). The affinities of the wild-type (WT) and mutants of the 14-3-3 ζ protein with PPD were measured with BLI (Fig. 5B) and the mutant forms of 14-3-3 ζ (Fig. 5C−E). As shown in Fig. 5F, the K_D of WT and three mutants with PPD were $4.52 \pm 0.12E$-

5 M, $2.35 \pm 0.11E$-3 M, $2.28 \pm 0.10E$-4 M, $1.36 \pm 0.11E$-4 M, respectively. The affinities of all the three mutants with PPD were reduced compared with the that of WT, suggesting that the R56, R127, and Y128 residues are critical sites for the binding of PPD to 14-3-3 ζ.

4. Discussion

Identifying protein targets for natural products is very challenging but very significant for the understanding of their related functions. Some experimental approaches can be used to identify the protein targets of small molecules, and affinity chromatography remains one of the most selective and versatile forms [35,36]. In comparison with other newly developed target recognition methods [37], affinity chromatography only depends on the ability of the compounds binding to the target protein, instead of specific biological parameters (i.e., thermodynamic [38] or proteolytic [39] measurements) that are only useful for a subset of the compounds. However, affinity chromatography requires an active group on a small molecule that binds to the solid support; hence, spatial hindrance may occur around the active group and prevent the protein to interact with the ligands [40].

To address this issue, we used high-purity ginseng total saponins as the ligands, where the sugar attachment sites of
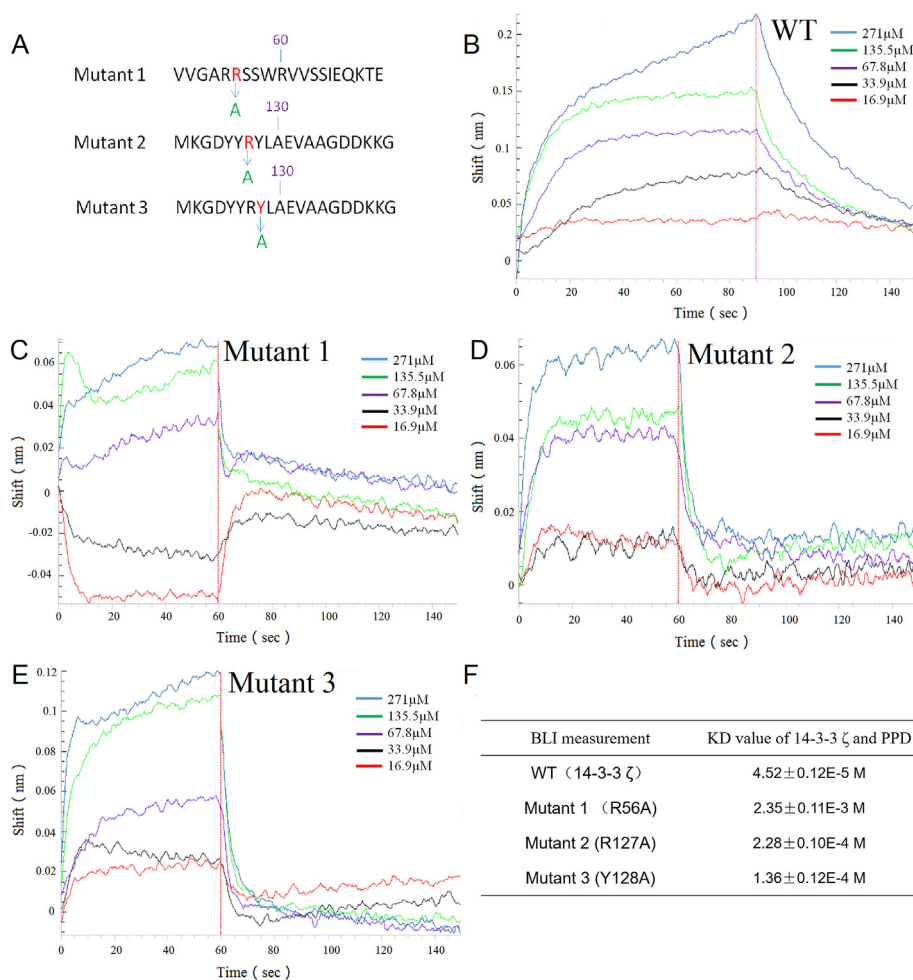

Fig. 5. R56, R127 and Y128 residues were necessary for the 14-3-3ζ protein to obtain affinity for PPD. (**A**) The mutant forms for 14-3-3 ζ protein, which arginine at position 56 is mutated to alanine (R56A, Mutant 1), arginine at position 127 is mutated to alanine (R127A,Mutant 2), and tyrosine at position 128 is mutated to alanine (Y128A, Mutant 3), were generated by site-directed mutagenesis. The affinity of PPD to 14-3-3 ζ protein (WT) (**B**), Mutant 1 (**C**), Mutant 2 (**D**) and Mutant 3 (**E**) were detected by BLI analysis. The association curve was generated after the Ni-NTA biosensors loaded with His-tagged 14-3-3 ζ protein and then incubated with PPD. (**F**) K_D values of WT and Mutants indicated that three residues were critical for the PPD binding to 14-3-3 ζ protein. The results presented are representative of at least three experiments. Data are expressed as mean ± S.E.M. (n = 3).

ginsenosides at C-3, C-6, or C-20 positions are different from each other [3]. From the initial screening, we identified five proteins as potential targets for ginsenosides in brain tissues, including the 14-3-3 ζ protein, the 14-3-3 ε protein, actin, creatine kinase B-type, and ATP synthase subunit beta. Among these proteins, creatine kinase has been identified and reported in our previous study [3]. ATP synthase subunit beta is involved in the last step of oxidative phosphorylation of the respiratory chain, which is mainly related to energy. The 14-3-3 proteins are a group of acidic soluble proteins (27-32 kDa) with the highest abundance in the brain [41]. In recent years,14-3-3 proteins have drawn increasing attention as effective drug targets of various diseases. More binding partners, mostly polypeptides, for 14-3-3 are found to be effective for 14-3-3 related increases. 14-3-3 ζ plays key roles, such as synaptic plasticity, learning and memory, and neuronal differentiation, in the CNS [42]. Natural products act as valuable sources of drugs and lead structures for new drug discovery, but many of their direct protein targets remain unknown. We applied the BLI technique to detect the direct interaction of 14-3-3 ζ to parent ginsenosides (i.e., Rd, Rb1, Re, and Rg1) and their metabolites (i.e., Rh2, Rh1, F1, PPT, CK, and PPD) (Fig. 3A and B). In subsequent research, we chose PPD, the most potent ligand among all the compounds tested, to study the interaction with the 14-3-3 ζ protein. The BLI kinetics analysis (Fig. 3C) and ITC assays (Fig. 3D) both showed that PPD had the modest binding affinity to the 14-3-3 ζ protein. Crystallographic study showed that PPD directly bind to the active site of the 14-3-3 ζ protein and the main interactions occurred between the residues R56, R127, and Y128 of the 14-3-3 ζ protein and a portion of PPD (Fig. 4). Moreover, mutating any of the above residues resulted in a significant decrease of affinity between PPD and the 14-3-3 ζ protein(Fig. 5). These results indicate that 14-3-3 ζ is a cellular target of PPD, and R56, R127, and Y128 residues are located in the binding site.

The 14-3-3 proteins are involved in many types of neural processes, such as learning and memory and synaptic function [43]. The 14-3-3 ζ protein is related to various neurological diseases and signaling pathways. For example, the isotype 14-3-3 ζ causes the oligomerization of its target proteins (such as phosphorylated tau), and high levels of 14-3-3 ζ increase the levels of phosphorylated tau, which is a marker associated with Alzheimer's disease [44]. The 14-3-3 ζ protein is localized in amyloid plaques in human brains with spongiform encephalopathies [41]. In the spinal cerebellar ataxia type 1 (SCA1) of polyglutamine repetitive disease, after Akt phosphorylation, 14-3-3 ζ could bind to and stabilize ataxin-1, thereby slowing its normal degradation [45]. Li et al [46] demonstrated that 14-3-3 ζ mediated tau phosphorylation in HEK-293 cells by Ser9-phosphorylated GSK3β. In summary, it is possible that ginsenosides and their metabolites may exert their neural activities based on 14-3-3ζ protein. In this study, we report the first crystal structure of a natural compound PPD in complex with its target protein 14-3-3 ζ. Further investigation of binding properties by co-crystallization and amino acid site-directed mutation confirmed the binding site on 14-3-3 ζ [47]. However, how the PPD exerts neural activity through 14-3-3 ζ needs further investigation.

5. Conclusion

In this study, we demonstrated that the 14-3-3 ζ protein is a target protein of ginsenosides in brain tissues. The metabolites of ginsenosides could be directly bound to the 14-3-3 ζ protein, among which PPD displayed the highest affinity. Our findings help to better understand the mechanisms of ginseng neuronal activities and generate relevant implications in developing small-molecule compounds that can bind to 14-3-3 ζ based on the structure of

dammarane-type triterpenoid with a four trans-ring rigid steroid skeleton.

Conflicts of interest

The authors have declared that there is no conflict of interest.

Appendix A. Supplementary data

Supplementary data to this article can be found online at https://doi.org/10.1016/j.jgr.2020.12.007.

Contributors

F·C., J.Z. and Y.Z. conceived and designed the experiments. F.C., L.C. and W.L. performed the experiments. F.C., L.C., W.L., Z.Z., J.L., W.Z., Z.Z., J.Z., and Y.Z. analyzed the data and drafted the manuscript. All authors contributed to the revision of this manuscript and approved the final manuscript.

References

[1] Smith I, Williamson EM, Putnam S, Farrimond J, Whalley BJ. Effects and mechanisms of ginseng and ginsenosides on cognition. Nutr Rev 2014;72(5):319—33.
[2] Shi ZY, Zeng JZ, Wong AST. Chemical structures and pharmacological profiles of ginseng saponins. Molecules 2019;24(13):2443.
[3] Chen FY, Zhu KX, Chen L, Ouyang LF, Chen CH, Gu L, Jiang YC, Wang ZL, Lin ZX, Zhang Q, et al. Protein target identification of ginsenosides in skeletal muscle tissues: discovery of natural small-molecule activators of muscle-type creatine kinase. J Ginseng Res 2020;44:461—74.
[4] Li XX, Zhang CC, Xiong YK. Advances in pharmacokinetics of ginsenosides. Chin Pharm J 2012;47(14):1101—4.
[5] Yang XW. Pharmacokinetic studies of chemical constituents of ginseng. Mod Chin Med 2016;18(1):16—35.
[6] Qi LW, Wang CZ, Du GJ, Zhang ZY, Calway T, Yuan CS. Metabolism of ginseng and its interactions with drugs. Curr Drug Metab 2011;12(9):818—22.
[7] Peng D, Wang H, Qu C, Xie L, Wicks SM, Xie J. Ginsenoside Re: its chemistry, metabolism and pharmacokinetics. Chin Med 2012;7:2.
[8] Liu MY, Wang HT, Zhao SH, Shi XW, Zhang YF, Xu HH, Wang YF, Li XJ, Zhang LT. Studies on target tissue distribution of ginsenosides and epimedium flavonoids in rats after intravenous administration of Jiweiling freeze-dried powder. Biomed Chromatogr 2011;25(11):1260—72.
[9] Chen C, Wang LS, Cao FR, Miao XQ, Chen TK, Chang Q, Zheng Y. Formulation of 20(S)-protopanaxadiol nanocrystals to improve oral bioavailability and brain delivery. Int J Pharm 2016;497:239—47.
[10] Jin S, Jeon JH, Lee S, Kang WY, Seong SJ, Yoon YR, Choi MK, Song IS. Detection of 13 ginsenosides (Rb1, Rb2, Rc, Rd, Re, Rf, Rg1, Rg3, Rh2, F1, compound K, 20(S)-Protopanaxadiol, and 20(S)-Protopanaxatriol) in human plasma and application of the analytical method to human pharmacokinetic studies following two week-repeated administration of red ginseng extract. Molecules 2019;24(14):2618.
[11] Rokot NT, Kairupan TS, Cheng KC, Runtuwene J, Kapantow NH, Amitani M, Morinaga A, Amitani H, Asakawa A, Inui A. A role of ginseng and its constituents in the treatment of central nervous system disorders. Evid Based Complement Alternat Med 2016;2016:2614742.
[12] Zheng MM, Xin YZ, Li YJ, Xu FX, Xi XZ, Guo H, Cui XW, Cao H, Zhag X, Han CC. Ginsenosides: a potential neuroprotective agent. Biomed Res Int 2018;2018:8174345.
[13] Wang PP, Wei YJ, Fan Y, Liu QF, Wei W, Yang CS, Zhang L, Zhao GP, Yue JM, Yan X, et al. Production of bioactive ginsenosides Rh2 and Rg3 by metabolically engineered yeasts. Metab Eng 2015;29:97—105.
[14] Zheng SW, Xiao SY, Wang J, Hou W, Wang YP. Inhibitory effects of ginsenoside ro on the growth of B16F10 melanoma via its metabolites. Molecules 2019;24(16):2985.

[15] Zhang HL, Li Z, Zhou ZL, Yang HY, Zhong ZY, Lou CX. Antidepressant-like effects of ginsenosides: a comparison of ginsenoside Rb3 and its four deglycosylated derivatives, Rg3, Rh2, compound K, and 20(S)-protopanaxadiol in mice models of despair. Pharmacol Biochem Behav 2016;140:17–26.

[16] Chen W, Guo YJ, Yang WJ, Zheng P, Zeng JS, Tong WS. Protective effect of ginsenoside Rb1 on integrity of blood-brain barrier following cerebral ischemia. Exp Brain Res 2015;233(10):2823–31.

[17] Zhu G, Wang Y, Li J, Wang J. Chronic treatment with ginsenoside Rg1 promotes memory and hippocampal long-term potentiation in middle-aged mice. Neuroscience 2015;292:81–9.

[18] Hou JG, Xue JJ, Lee M, Liu L, Zhang DL, Sun MQ, Zheng YN, Sung CK. Ginsenoside Rh2 improves learning and memory in mice. J Med Food 2013;16(8):772–6.

[19] Lomenick B, Olsen RW, Huang J. Identification of direct protein targets of small molecules. ACS Chem Biol 2011;6(1):34–46.

[20] Zhao YN, Wang ZL, Dai JG, Chen L, Huang YF. Preparation and quality assessment of high-purity ginseng total saponins by ion exchange resin combined with macroporous adsorption resin separation. Chin J Nat Med 2014;12(5):382–92.

[21] Ouyang LF, Wang ZL, Dai JG, Chen L, Zhao YN. Determination of total ginsenosides in ginseng extracts using charged aerosol detection with post-column compensation of the gradient. Chin J Nat Med 2014;12(11):857–68.

[22] Joo EJ, Ha YW, Shin H, Son SH, Kim YS. Generation and characterization of monoclonal antibody to ginsenoside rg3. Biol Pharm Bull 2009;32(4):548–52.

[23] Wang YS, Zhang B, Zhu J, Yang CL, Guo Y, Liu CL, Liu F, Huang HQ, Zhao SW, Liang Y, et al. Molecular basis for the final oxidative rearrangement steps in chartreusin biosynthesis. J Am Chem Soc 2018;140(34):10909–14.

[24] Lountos GT, Zhao XZ, Kiselev E, Tropea JE, Needle D, Pommier Y, Burke TR, Waugh DS. Identification of a ligand binding hot spot and structural motifs replicating aspects of tyrosyl-DNA phosphodiesterase I (TDP1) phosphoryl recognition by crystallographic fragment cocktail screening. Nucleic Acids Res 2019;47(19):10134–50.

[25] Zhang B, Wang KB, Wang W, Wang X, Liu F, Zhu J, Shi J, Li LY, Han H, Xu K, et al. Enzyme-catalysed [6+4] cycloadditions in the biosynthesis of natural products. Nature 2019;568(7750):122–6.

[26] Curran EC, Wang H, Hinds TR, Zheng N, Wang EH. Zinc knuckle of TAF1 is a DNA binding module critical for TFIID promoter occupancy. Sci Rep 2018;8(1):4630.

[27] Wang YS, Lin Y, Li H, Li Y, Song Z, Jin YH. The identification of molecular target of (20S) ginsenoside Rh2 for its anti-cancer activity. Sci Rep 2017;7(1):12408.

[28] Lu Y, Ding S, Zhou R, Wu J. Structure of the complex of phosphorylated liver kinase B1 and 14-3-3zeta. Acta Crystallogr F Struct Biol Commun 2017;73:196–201.

[29] Battye TG, Kontogiannis L, Johnson O, Powell HR, Leslie AG. iMOSFLM: a new graphical interface for diffraction-image processing with MOSFLM. Acta Crystallogr D Biol Crystallogr 2011;67:271–81.

[30] McCoy AJ, Grosse-Kunstleve RW, Adams PD, Winn MD, Storoni LC, Read RJ. Phaser crystallographic software. J Appl Crystallogr 2007;40:658–74.

[31] Adams PD, Afonine PV, Bunkóczi G, Chen VB, Davis IW, Echols N, Headd JJ, Hung LW, Kapral GJ, Grosse-Kunstleve RW, et al. PHENIX: a comprehensive Python-based system for macromolecular structure solution. Acta Crystallogr D Biol Crystallogr 2010;66:213–21.

[32] Emsley P, Lohkamp B, Scott WG, Cowtan K. Features and development of Coot. Acta Crystallogr D Biol Crystallogr 2010;66:486–501.

[33] Moustakim M, Riedel K, Schuller M, Gehring AP, Monteiro OP, Martin SP, Fedorov O, Heer J, Dixon DJ, Elkins JM, et al. Discovery of a novel allosteric inhibitor scaffold for polyadenosine-diphosphate-ribose polymerase 14 (PARP14) macrodomain 2. Bioorg Med Chem 2018;26(11):2965–72.

[34] Furukawa A, Kakita K, Yamada T, Ishizuka M, Sakamoto J, Hatori N, Maeda N, Ohsaka F, Saitoh T, Nomura T, et al. Structural and thermodynamic analyses reveal critical features of glycopeptide recognition by the human PILRalpha immune cell receptor. J Biol Chem 2017;292(51):21128–36.

[35] Park KD, Kim D, Reamtong O, Eyers C, Gaskell SJ, Liu R, Kohn H. Identification of a lacosamide binding protein using an affinity bait and chemical reporter strategy: 14-3-3 zeta. J Am Chem Soc 2011;133(29):11320–30.

[36] Hage DS, Matsuda R. Affinity chromatography: a historical perspective. Methods Mol Biol 2015;1286:1–19.

[37] Futamura Y, Muroi M, Osada H. Target identification of small molecules based on chemical biology approaches. Mol Biosyst 2013;9(5):897–914.

[38] Huber KV, Olek KM, Muller AC, Tan CS, Bennett KL, Colinge J, Superti-Furga G. Proteome-wide drug and metabolite interaction mapping by thermal-stability profiling. Nat Methods 2015;12(11):1055–7.

[39] Pai MY, Lomenick B, Hwang H, Schiestl R, McBride W, Loo JA, Huang J. Drug affinity responsive target stability (DARTS) for small-molecule target identification. Methods Mol Biol 2015;1263:287–98.

[40] Chang J, Kim Y, Kwon HJ. Advances in identification and validation of protein targets of natural products without chemical modification. Nat Prod Rep 2016;33(5):719–30.

[41] Zhou XY, Hu DX, Chen RQ, Chen XQ, Dong WL, Yi CL. 14-3-3 isoforms differentially regulate NFkappaB signaling in the brain after ischemia-reperfusion. Neurochem Res 2017;42(8):2354–62.

[42] Dai JG, Murakami K. Constitutively and autonomously active protein kinase C associated with 14-3-3 zeta in the rodent brain. J Neurochem 2003;84(1):23–34.

[43] Toyo-oka K, Wachi T, Hunt RF, Baraban SC, Taya S, Ramshaw H, Kaibuchi K, Schwarz QP, Lopez AF, Wynshaw-Boris A. 14-3-3epsilon and zeta regulate neurogenesis and differentiation of neuronal progenitor cells in the developing brain. J Neurosci 2014;34(36):12168–81.

[44] Deng Y, Jiang B, Rankin CL, Toyo-Oka K, Richter ML, Maupin-Furlow JA, Moskovitz J. Methionine sulfoxide reductase A (MsrA) mediates the ubiquitination of 14-3-3 protein isotypes in brain. Free Radic Biol Med 2018;129:600–7.

[45] Mackie S, Aitken A. Novel brain 14-3-3 interacting proteins involved in neurodegenerative disease. Febs J 2005;272(16):4202–10.

[46] Li T, Paudel HK. 14-3-3zeta facilitates GSK3beta-catalyzed tau phosphorylation in HEK-293 cells by a mechanism that requires phosphorylation of GSK3beta on Ser9. Neurosci Lett 2007;414(3):203–8.

[47] Cromm PM, Wallraven K, Glas A, Bier D, Furstner A, Ottmann C, Grossmann TN. Constraining an irregular peptide secondary structure through ring-closing alkyne metathesis. Chembiochem 2016;17(20):1915–9.